

# High-resolution photoinduced transient spectroscopy of radiation defect centres in silicon

**Paweł Kamiński**

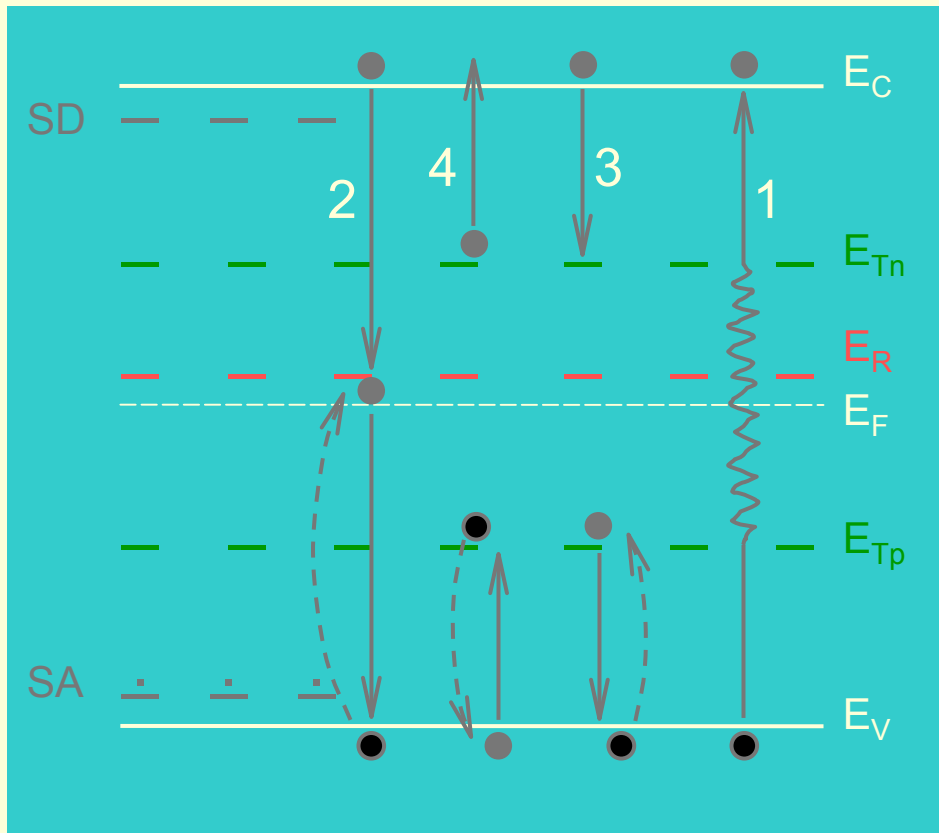
*Institute of Electronic Materials Technology,  
133 Wólczyńska Str. 01-919 Warszawa, Poland  
e-mail: [pawel.kaminski@itme.edu.pl](mailto:pawel.kaminski@itme.edu.pl)*

## Outline

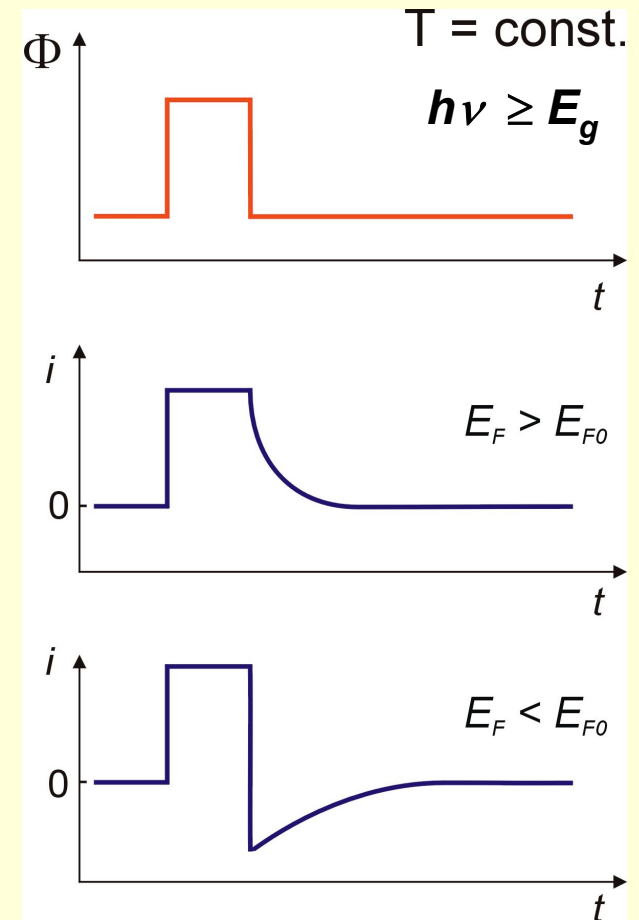
- PITS: basics, advantages and limitations
- Experimental details: samples, measuring system
- Analysis of photocurrent relaxation waveforms
- HRPITS spectra for radiation defects in bulk silicon
- Images of spectral fringes for radiation defects in epitaxial silicon
- Conclusions

# PITS Basics

- High-Resolution Photoinduced Transient Spectroscopy (HRPITS) - for high-resistivity materials ( $10^3 - 10^{10} \Omega\text{cm}$ )



1. Generation
2. Recombination
3. Trapping
4. Emission



## HRPITS advantages (1)

- The method is dedicated to study defect centres in high-resistivity materials, in particular in silicon with a resistivity above 10 k $\Omega$ cm after irradiation with high fluences of high-energy hadrons. The signature of a defect, represented by the temperature dependence of the emission rate of charge carriers, is determined and the activation energy ( $E_a$ ) and pre-exponential factor in the Arrhenius equation ( $A$ ) are obtained. The **concentration** of defect centres can also be estimated.
- High sensitivity – the minimal concentration of defect centres which can be detected is of the order 10<sup>10</sup> cm<sup>-3</sup>.
- The charge carriers are captured by defect centres and emitted to the conduction or valance band at the same temperature, similarly as in DLTS technique.
- The temperature dependence of the emission rate of charge carriers can be determined using the correlation procedure (double box-car analysis), similarly as in DLTS technique. The correlation spectra can be produced in a wide range of emission rate windows from 10 to 10<sup>5</sup> s<sup>-1</sup>.

## HRPITS advantages (2)

- Advanced computational procedures can be applied to extracting, with a high resolution, the parameters of defect centres from the photocurrent relaxation waveforms. Images of the material defect structure showing the temperature dependences of emission rate for detected defect centres and differences in the centres concentrations can be created.
- Measurements are performed at low electric fields, around 300 V/cm, slightly affecting the potential barrier around defect.
- Concentration of shallow impurities has small influence on the measured values.
- Averaging can be effectively used to significantly reduce the noise in the photocurrent relaxation waveforms. Usually, the transient recorded at a given temperature represents an average of minimum 500 transients. This results in the high signal to noise ratio.

## HRPITS limitations

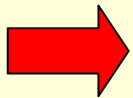
- It is impossible to distinguish directly electron and hole traps.
- It is impossible to distinguish directly acceptor and donor centres.
- We have no direct information on the atomic configuration of defect centre.
- There is strong effect of the photon flux on the photocurrent relaxation.
- Measurements are fairly time-consuming.

# Samples

- Pieces of wafers of bulk silicon or with epitaxial layer – preferable dimensions  $1 \times 1 \text{ cm}^2$ , possible size  $0.5 \times 0.7 \text{ cm}^2$ .
- The sample surface should be of good quality.
- Detector structures can be used after removing the top  $p^+$  layer.
- Two co-planar ohmic contacts are deposited on the wafer surface. Contact dimensions  $2.1 \times 2.1 \text{ mm}^2$ ; distance between contacts 0.7 mm.

# Typical experimental conditions of HRPITS measurements

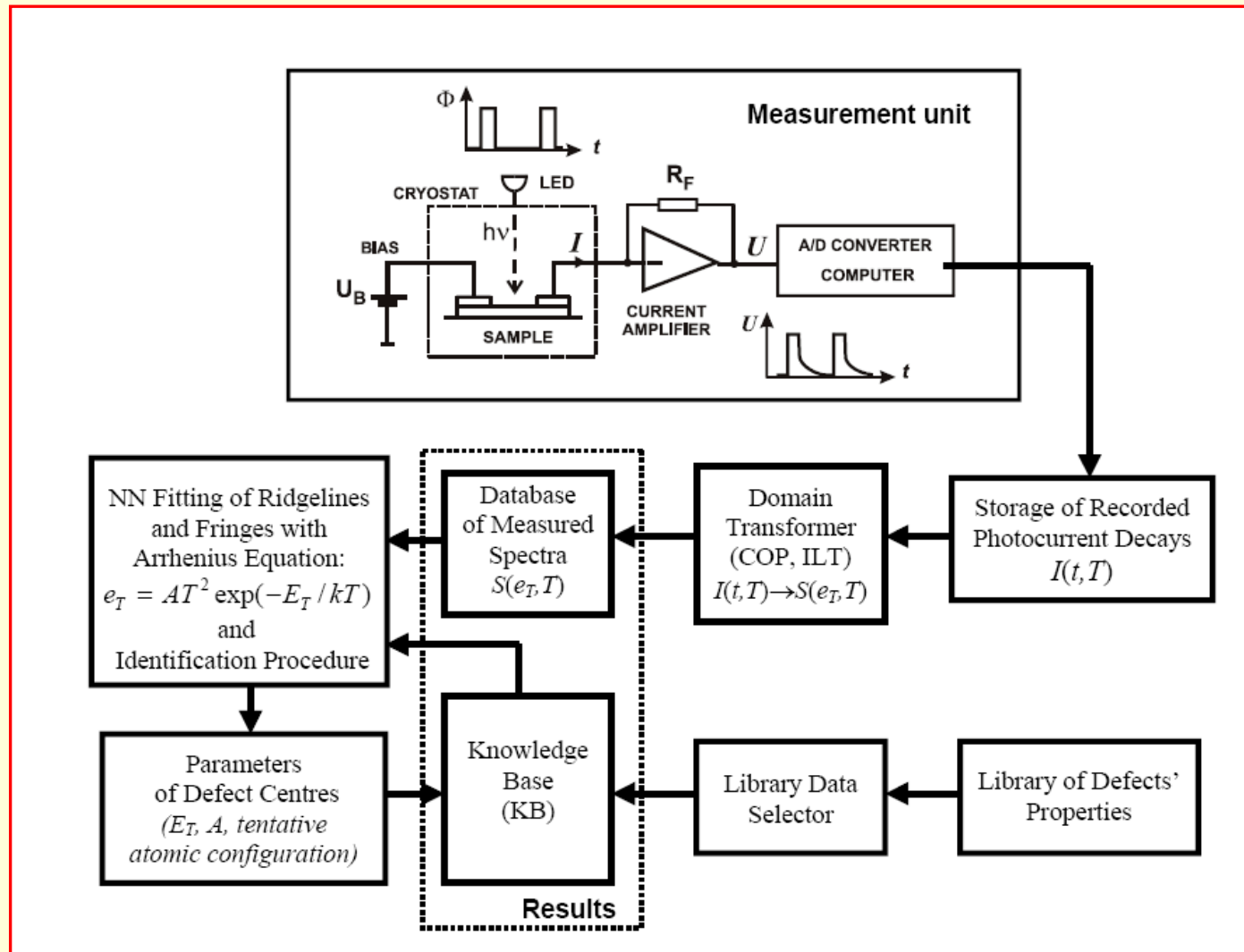
- Light Source : 5 mW / 650 nm laser
- Bias: 10 V
- Temperature range: 20 - 320 K
- Temperature step: 2 K
- Excitation pulse width: 50 ms
- Repetition time: 300 ms
- Rise time: 10  $\mu$ s
- Gain:  $10^5 - 10^9$  V/A



150 photocurrent transients are digitally recorded with 12-bit amplitude resolution and 1- $\mu$ s time resolution. Each transient consists of 350000 data points. Analysis of the photocurrent relaxation waveforms is performed by means of the correlation procedure and inverse Laplace transform (ILT) algorithm .



# HRPITS technique - experimental system



# Model of Photocurrent Relaxation Waveforms

$$i_m(t, T) = I_m(\lambda, T) \exp(-e_{Tm}t);$$

$$I_m(\lambda, T) = n_{tom}(T) e_{Tm}(T) \mu_T(T) \tau_T(T) C(\lambda, T) qE$$

$$i(t, T) = \sum_{m=1}^M I_k(\lambda, T) \exp(-e_{Tm}t);$$

$$e_{Tm} = A_m T^2 \exp(-E_m / k_B T)$$

$$A_{mn} = \gamma_n \sigma_{mn} ; A_{mp} = \gamma_p \sigma_{mp}$$


For Si

$$\gamma_n = 1.07 \times 10^{21} \text{ cm}^{-2}\text{K}^{-2}\text{s}^{-1} ; \gamma_p = 2.64 \times 10^{21} \text{ cm}^{-2}\text{K}^{-2}\text{s}^{-1}$$

# Procedures for analysis of the photocurrent relaxation waveforms

## Correlation procedure:

$$S_{Kg}(T_j) = C \int_0^{t_w} \frac{i(t, T_j)}{i(0, T_j) - i(t_{end}, T_j)} w_g(t) dt, \quad j = 1..J, \quad g = 1..G$$

 The spectral surface formed by the set of one dimensional spectra  $S_{Kg}(T_j)$  for  $G$  emission rate windows  $e_{Tg}$

$$w_g(t) = \delta(t - t_{2g}) - \delta(t - t_{1g})$$

$$S_{Kg}(T_j) = [i(t_{2g}, T_j) - i(t_{1g}, T_j)] / [i(0, T_j) - i(t_{end}, T_j)], \quad j = 1..J; \quad t_2 / t_1 = 3, \quad e_{Tg} = 1.23 / t_{1g}$$

Inverse Laplace transformation algorithm:  $i(t) = \int_0^\infty S_L(e_T) \exp(-e_T t) de_T; T_j$

in discrete form  $i(t) = \sum_{m=1}^M c_m S_L(e_{Tm}) \exp(-e_{Tm} t)$  and matrix equation  $i = K S_L$ ,

with matrix elements  $K = [\exp(-e_{Tm} t_r)]_{m=1..M}^{r=1..R}$

**Neural network approximation:** The neural approximator has the form of two-layered perceptron whose inputs are the arguments of the spectral surface. The activation function of hidden neurons is assumed as a weighted sum of two-sigmoid functions. Hence, each hidden neuron can model the lateral surface of the two-dimensional spectrum. When added together, they create the fold that matches the experimental fold corresponding to a specific defect centre. The parameters of this centre, such as activation energy and apparent capture cross section, are directly obtained as the weight coefficients of hidden neurons by means of a certain optimization process.

# 10- MeV proton irradiated samples

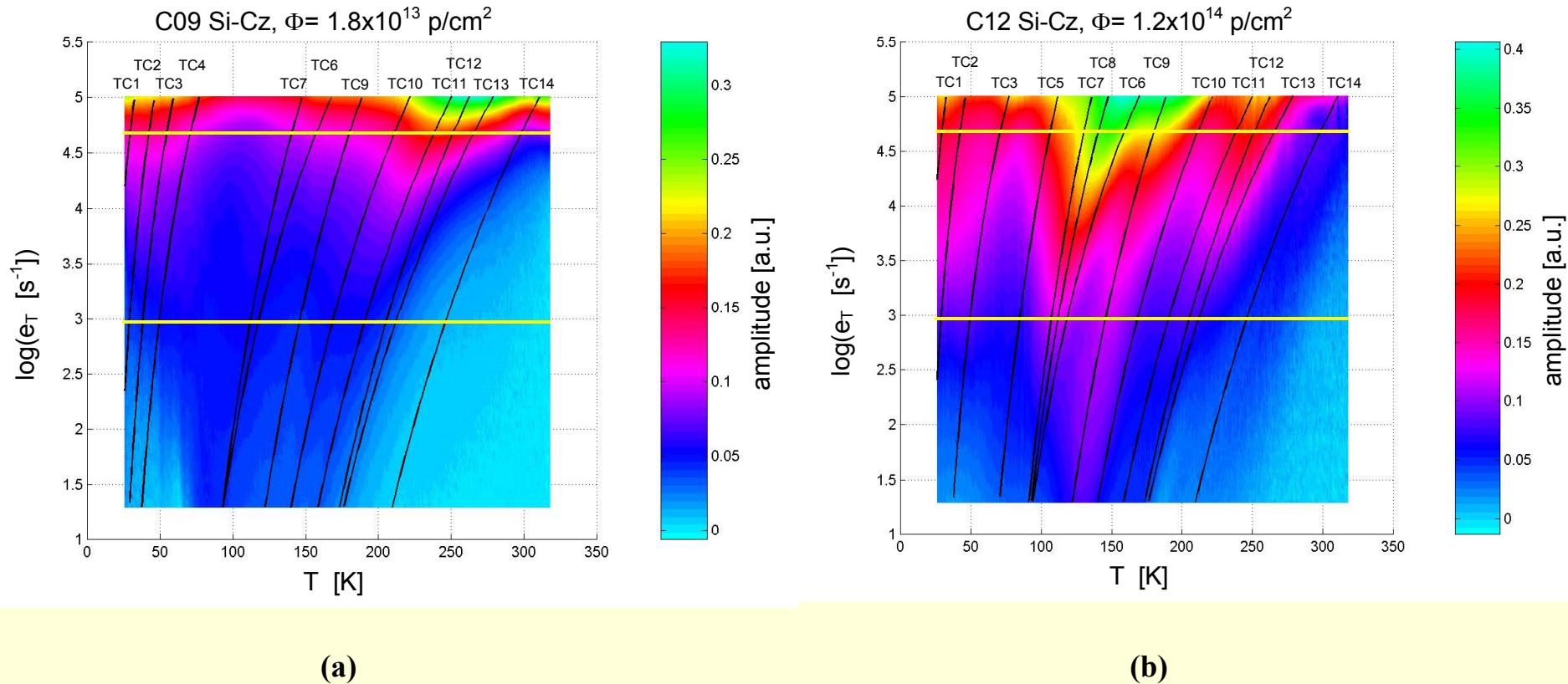
## A. High-resistivity bulk Si grown by the Czochralski method in magnetic field, Okmetic

Sample	Fluence (p/cm <sup>2</sup> )	n at 300 K (cm <sup>-3</sup> )	Resistivity at 300 K (Ωcm)	Hall mobility at 300 K (cm <sup>2</sup> /Vs)	Type
C00	non- irradiated	3.6x10 <sup>12</sup>	1.08x10 <sup>3</sup>	1585	n
C09	1.8x10 <sup>13</sup>	5.8X10 <sup>10</sup>	1.1x10 <sup>5</sup>	959	n
C12	1.2x10 <sup>14</sup>	6.0x10 <sup>10</sup>	9.6x10 <sup>4</sup>	1094	n

## B. High-resistivity FZ Si, Topsil

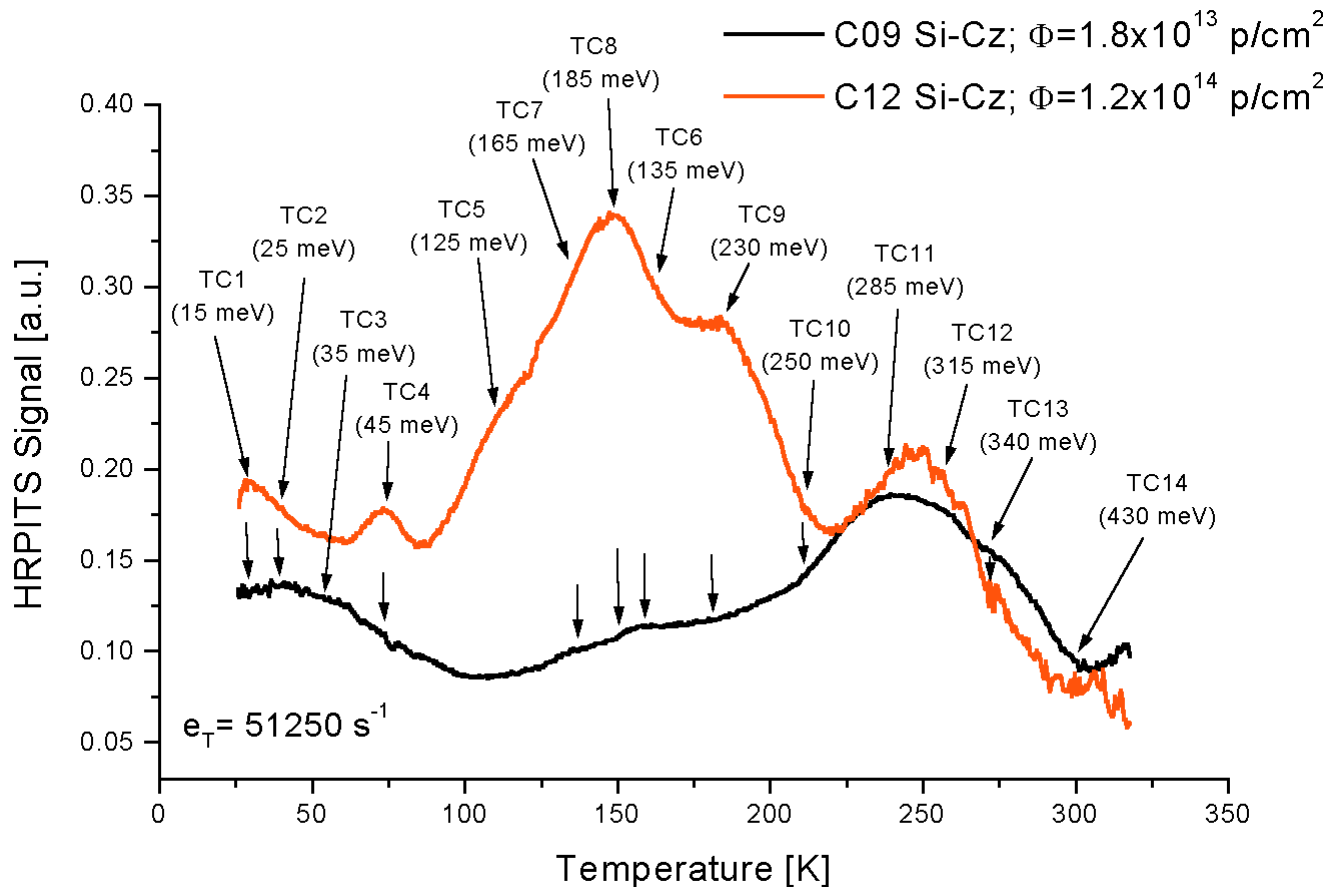
Sample	Fluence (p/cm <sup>2</sup> )	n at 300 K (cm <sup>-3</sup> )	Resistivity at 300 K (Ωcm)	Hall mobility at 300 K (cm <sup>2</sup> /Vs)	Type
T00	non- irradiated	1.5x10 <sup>12</sup>	2.8x10 <sup>3</sup>	1600	n
T09	1.8x10 <sup>13</sup>	5.8X10 <sup>10</sup>	1.1x10 <sup>5</sup>	967	n
T12	1.2x10 <sup>14</sup>	4.4x10 <sup>10</sup>	1.7x10 <sup>5</sup>	848	n

# Effect of proton fluence on defect structure of Czochralski-grown Si



**Experimental spectral fringes obtained as a result of the correlation procedure for defect centres detected in Cz-Si irradiated with fluences of  $1.8 \times 10^{13} \text{ p/cm}^2$  (a) and  $1.2 \times 10^{14} \text{ p/cm}^2$  (b). The solid lines illustrate the temperature dependences of emission rate determined by means of advanced computational analysis for detected defect centres.**

# Effect of proton fluence on defect structure of Czochralski-grown Si

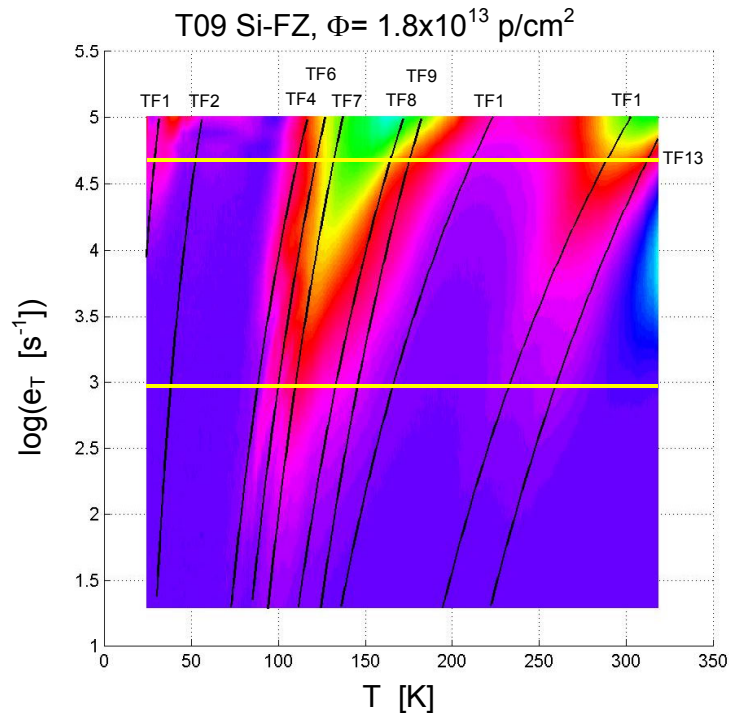


Comparison of 1-D HRPITS spectra obtained as a result of the correlation procedure for high-resistivity Cz-Si samples after 10-MeV proton irradiation with fluences of  $1.8 \times 10^{13}$  and  $1.2 \times 10^{14} \text{ p/cm}^2$ .

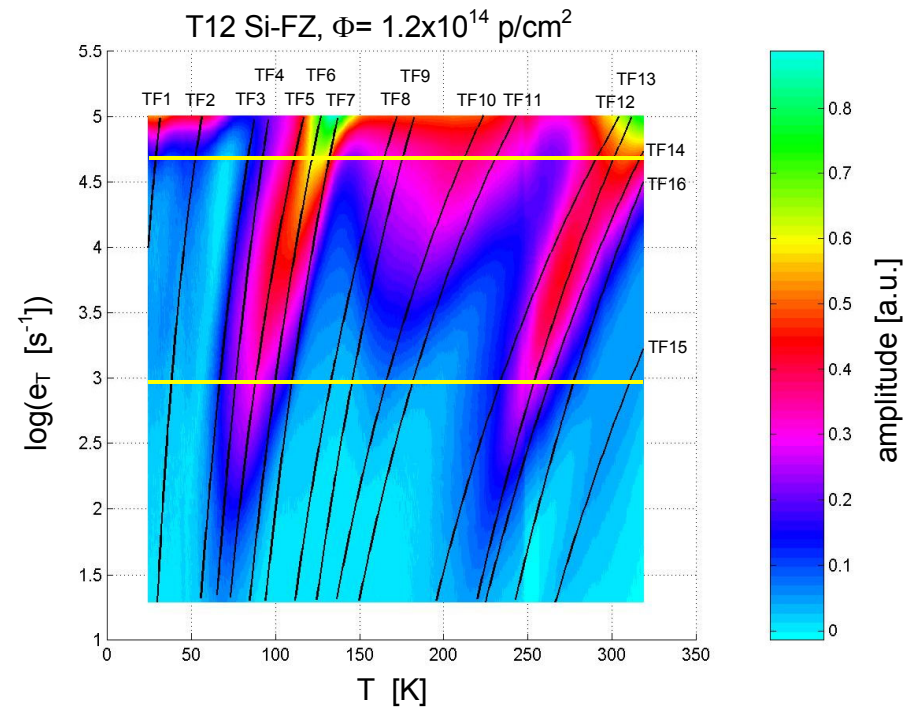
Summary of the properties and concentrations of defect centres detected by the HRPITS method in high-resistivity Cz-Si after 10-MeV proton irradiation with fluences of  $1.8 \times 10^{13}$  and  $1.2 \times 10^{14}$  p/cm<sup>2</sup>

Trap label	$E_a$ [meV]	$A$ [s <sup>-1</sup> K <sup>-2</sup> ]	$\sigma_e$ or $\sigma_h$ [cm <sup>2</sup> ]	Trap concentration $N_T$ [cm <sup>-3</sup> ]		Identification/ Remarks
				$\Phi=1.8 \times 10^{13}$ [p/cm <sup>2</sup> ]	$\Phi=1.2 \times 10^{14}$ [p/cm <sup>2</sup> ]	
TC1	15	$2.0 \times 10^4$	$1.9 \times 10^{-17}$	$1.9 \times 10^{14}$	$2.3 \times 10^{14}$	shallow donor ; $e$
TC2	25	$2.5 \times 10^4$	$2.4 \times 10^{-17}$	$3.2 \times 10^{14}$	$4.0 \times 10^{14}$	shallow donor ; $e$
TC3	35	$2.7 \times 10^4$	$2.5 \times 10^{-17}$	$4.5 \times 10^{14}$	not observed	shallow donor ; $e$
TC4	45	$1.5 \times 10^4$	$1.4 \times 10^{-17}$	$7.4 \times 10^{14}$	$1.0 \times 10^{15}$	shallow donor ; $e$
TC5	125	$3.5 \times 10^6$	$3.3 \times 10^{-15}$	not observed	$2.1 \times 10^{15}$	$C_i^{-/0}$ ; $e$
TC6	135	$3.8 \times 10^4$	-	$1.2 \times 10^{15}$	$2.2 \times 10^{15}$	TX3, H-related ?
TC7	165	$2.0 \times 10^6$	$1.2 \times 10^{-15}$	$1.0 \times 10^{15}$	$2.1 \times 10^{15}$	$VO_i^{-/0} + C_iC_s(A)^{-/0}$ ; $e$
TC8	185	$4.0 \times 10^7$	$1.5 \times 10^{-14}$	not observed	$2.6 \times 10^{15}$	$V_2^{+/0}$ ; $h$
TC9	230	$4.0 \times 10^6$	$3.8 \times 10^{-15}$	$1.4 \times 10^{15}$	$2.9 \times 10^{15}$	$V_2^{2-/0}$ ; $e$
TC10	250	$1.0 \times 10^6$	$3.8 \times 10^{-16}$	$1.6 \times 10^{15}$	$1.8 \times 10^{15}$	$VOH^{+/0}$ ; $h$
TC11	285	$9.0 \times 10^5$	$3.4 \times 10^{-16}$	$1.9 \times 10^{15}$	$1.9 \times 10^{15}$	H-related; $h$
TC12	315	$6.0 \times 10^5$	$6.1 \times 10^{-16}$	$1.2 \times 10^{15}$	$1.6 \times 10^{15}$	E3 (H-related), $VOH^{-/0}$ ; $e$
TC13	340	$5.0 \times 10^6$	$1.9 \times 10^{-15}$	$1.8 \times 10^{15}$	$1.4 \times 10^{15}$	$C_iO_i^{+/0}$ or $C_iO_iV$ ; $h$
TC14	430	$1.0 \times 10^7$	$9.4 \times 10^{-15}$	$1.2 \times 10^{15}$	$9.6 \times 10^{14}$	$V_2^{-/0}$ ; $e$

# Effect of proton fluence on defect structure of FZ Si



(a)

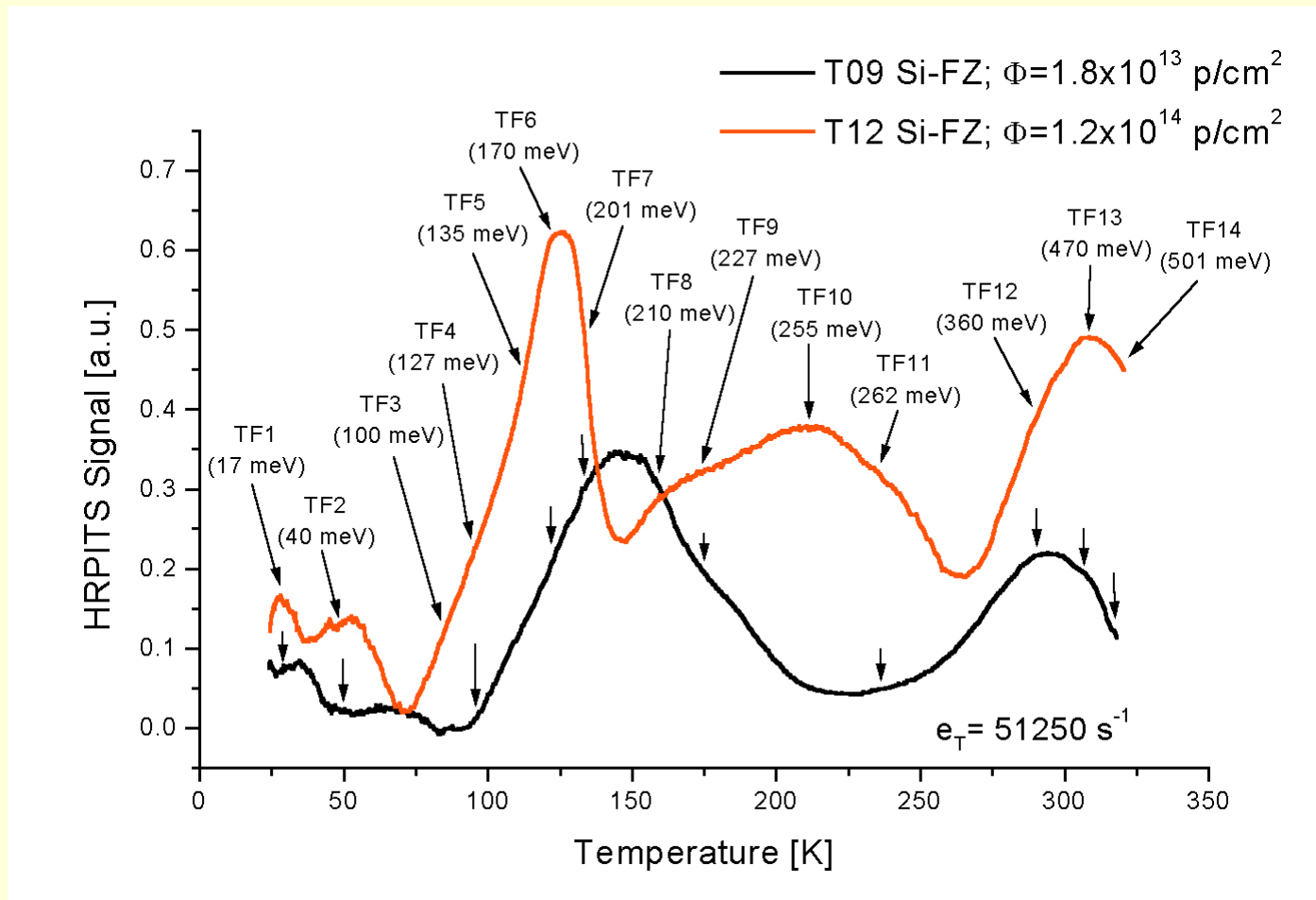


(b)

**Experimental spectral fringes obtained as a result of the correlation procedure for defect centres detected in FZ-Si irradiated with fluences of  $1.8 \times 10^{13} \text{ p/cm}^2$  (a) and  $1.2 \times 10^{14} \text{ p/cm}^2$  (b). The solid lines illustrate the temperature dependences of emission rate determined by means of advanced computational analysis for detected defect centres.**



# Effect of proton fluence on defect structure of FZ Si



Comparison of 1-D HRPITS spectra obtained as a result of the correlation procedure for high-resistivity FZ-Si samples after 10-MeV proton irradiation with fluences of  $1.8 \times 10^{13}$  and  $1.2 \times 10^{14} \text{ p/cm}^2$ .

Summary of the properties and concentrations of defect centres detected by the HRPITS method in high-resistivity FZ-Si after 10-MeV proton irradiation with fluences of  $1.8 \times 10^{13}$  and  $1.2 \times 10^{14}$  p/cm<sup>2</sup>

Trap label	$E_a$ [meV]	$A$ [s <sup>-1</sup> K <sup>-2</sup> ]	$\sigma_e$ or $\sigma_h$ [cm <sup>2</sup> ]	Trap concentration $N_T$ [cm <sup>-3</sup> ]		Identification/ Remarks
				$\Phi=1.8 \times 10^{13}$ [p/cm <sup>2</sup> ]	$\Phi=1.2 \times 10^{14}$ [p/cm <sup>2</sup> ]	
TF1	17	$5.2 \times 10^4$	$4.9 \times 10^{-17}$	$1.4 \times 10^{14}$	$2.1 \times 10^{14}$	shallow donor ; $e$
TF2	40	$1.2 \times 10^5$	$1.1 \times 10^{-16}$	$1.7 \times 10^{14}$	$4.6 \times 10^{14}$	shallow donor ; $e$
TF3	100	$7.2 \times 10^6$	$2.7 \times 10^{-15}$	not observed	$5.3 \times 10^{14}$	$C_i C_s(A)^{+/0}$ ; $h$
TF4	127	$2.2 \times 10^6$	$2.1 \times 10^{-15}$	$1.1 \times 10^{14}$	$9.0 \times 10^{14}$	$C_i^{-/0}$ ; $e$
TF5	135	$1.3 \times 10^8$	-	not observed	$2.3 \times 10^{15}$	self-interstitial agglomerate ( $I$ )
TF6	170	$3.5 \times 10^7$	$3.3 \times 10^{-14}$	$1.1 \times 10^{15}$	$3.4 \times 10^{15}$	$VO_i^{-/0} + C_i C_s(A)^{-/0}$ ; $e$
TF7	201	$1.3 \times 10^8$	$4.9 \times 10^{-14}$	$3.8 \times 10^{15}$	$3.1 \times 10^{15}$	$V_2^{+/0}$ ; $h$
TF8	210	$4.8 \times 10^6$	$4.5 \times 10^{-15}$	$2.9 \times 10^{15}$	$2.5 \times 10^{15}$	$E(115)$ ; $e$
TF9	227	$2.7 \times 10^5$	$2.5 \times 10^{-16}$	$1.2 \times 10^{15}$	$2.7 \times 10^{15}$	$V_2^{2+/+}$ ; $e$
TF10	255	$3.4 \times 10^5$	$1.3 \times 10^{-16}$	not observed	$3.6 \times 10^{15}$	$VOH^{+/0}$ ; $h$
TF11	262	$5.2 \times 10^7$	$2.0 \times 10^{-14}$	$8.6 \times 10^{14}$	$2.9 \times 10^{15}$	$C_i H^{+/0}$ ; $h$
TF12	360	$1.0 \times 10^6$	$3.8 \times 10^{-16}$	$3.3 \times 10^{15}$	$2.6 \times 10^{15}$	$C_i O_i^{+/0}$ or $C_i O_i V$ ; $h$
TF13	470	$1.9 \times 10^7$	$1.8 \times 10^{-14}$	$3.5 \times 10^{14}$	$5.6 \times 10^{15}$	$V_2^{-/0}$ ; $e$
TF14	501	$1.3 \times 10^8$	$4.9 \times 10^{-14}$	not observed	$3.2 \times 10^{15}$	H-related complex ; $h$
TF15	574	$2.0 \times 10^7$	$7.6 \times 10^{-15}$	not observed	$1.8 \times 10^{15}$	I-centre $(V_2 O)^{0/-}$ ; $h$
TF16	597	$8.7 \times 10^8$	$8.2 \times 10^{-13}$	not observed	$1.5 \times 10^{15}$	$E(325)$ , multivacancy, N, or H - related ; $e$

## Effect of proton fluence on formation of defect centres in Cz and FZ silicon - Summary of results (1)

- HRPITS technique with implementation of computational intelligence has been employed to studying the effect of fluence on defect structure of 10-MeV proton irradiated FZ and Cz silicon with starting net donor concentrations of  $1.5 \times 10^{12}$  and  $3.6 \times 10^{12} \text{ cm}^{-3}$ , respectively.
- The irradiation of Cz-Si with fluences of  $1.8 \times 10^{13}$  and  $1.2 \times 10^{14} \text{ p/cm}^2$  resulted in the formation of 12 and 14 defect centres, respectively, with activation energies ranging from 15 to 430 meV.
- For the lower fluence the predominant defects in Cz-Si were found to be an H-related complex (285 meV) and  $\text{C}_i\text{O}_i^{+/0}$  (340 meV).
- For the higher fluence the predominant defects in Cz-Si were found to be divacancies  $\text{V}_2^{2-/0}$  (230 meV) and  $\text{V}_2^{+/0}$  (185 meV).

## Effect of proton fluence on formation of defect centres in Cz and FZ silicon - Summary of results (2)

- The irradiation of FZ-Si with fluences of  $1.8 \times 10^{13}$  and  $1.2 \times 10^{14}$  p/cm<sup>2</sup> resulted in the formation of 10 radiation defects with activation energies ranging from 17 to 470 meV and 16 defects with activation energies in the range of 17-597 meV, respectively.
- For the lower fluence the predominant defects in FZ-Si were found to be the divacancy  $V_2^{+/0}$  (185 meV) and  $C_iO_i^{+/0}$  (340 meV).
- For the higher fluence the predominant defects in FZ-Si were found to be the divacancy  $V_2^{-/0}$  (470 meV) and  $VOH^{+/0}$  complex (255 meV).
- Comparison of the defect structure of Cz-Si and FZ-Si indicates that the defects occurring in the both materials after the irradiation with the lower fluence are:  $VO_i^{-/0} + C_iC_s(A)^{-/0}$ ,  $V_2^{2-/-}$ ,  $C_iO_i^{+/0}$  and  $V_2^{-/0}$ . For the higher fluence apart from these defects the common defects are:  $C_i^{-/0}$ ,  $V_2^{+/0}$ ,  $VOH^{+/0}$ .
- The irradiation of high-resistivity FZ-Si with a fluence of  $1.2 \times 10^{14}$  p/cm<sup>2</sup> results in the formation of midgap centres with activation energies 501, 574 and 597 meV attributed to an H-related complex,  $V_2O^{0/-}$  and an unidentified defect, respectively.

# Defect centres in epitaxial silicon irradiated with high proton fluences - Experimental details

## ITME: fabrication of epitaxial layer

1. Starting material: <111>, low resistivity ( $\rho < 0.02 \text{ } \Omega \cdot \text{cm}$ )  
300  $\mu\text{m}$  thick Czochralski (Cz) silicon substrate  
doped by Sb donors.
2. Thin (75  $\mu\text{m}$ ) medium resistivity ( $\rho = 50 \text{ } \Omega \cdot \text{cm}$ ),  
epitaxial silicon layers doped by P donors  
have been grown on the CZ-Si substrates forming  
simple n-n<sup>+</sup> structures.

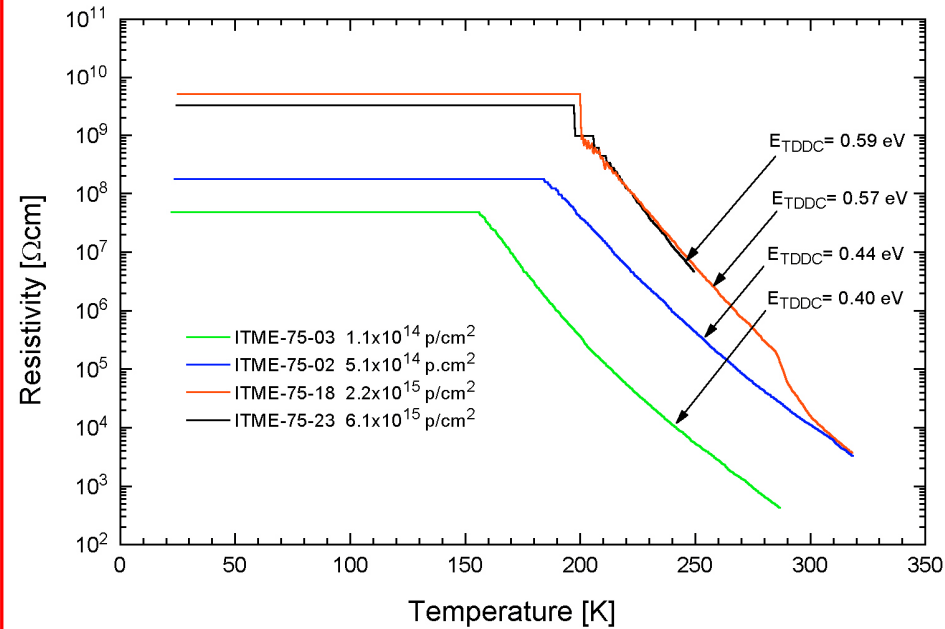
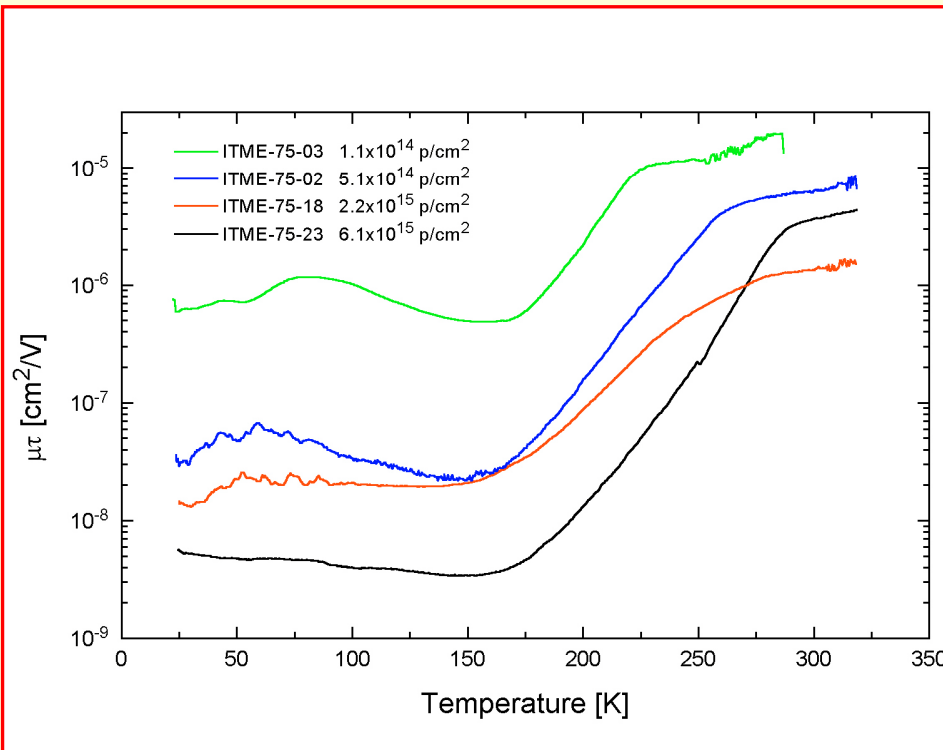
## CERN: 24- GeV/c proton irradiation; PS RUN period: P1A-2004

### Fluences

- $1.06 \times 10^{14} \text{ p/cm}^2$  - sample A
- $5.05 \times 10^{14} \text{ p/cm}^2$  - sample B
- $2.17 \times 10^{15} \text{ p/cm}^2$  - sample C
- $6.10 \times 10^{15} \text{ p/cm}^2$  - sample D

After the irradiation all the samples were stored at -20 °C.

# Epitaxial silicon irradiated with high proton fluences

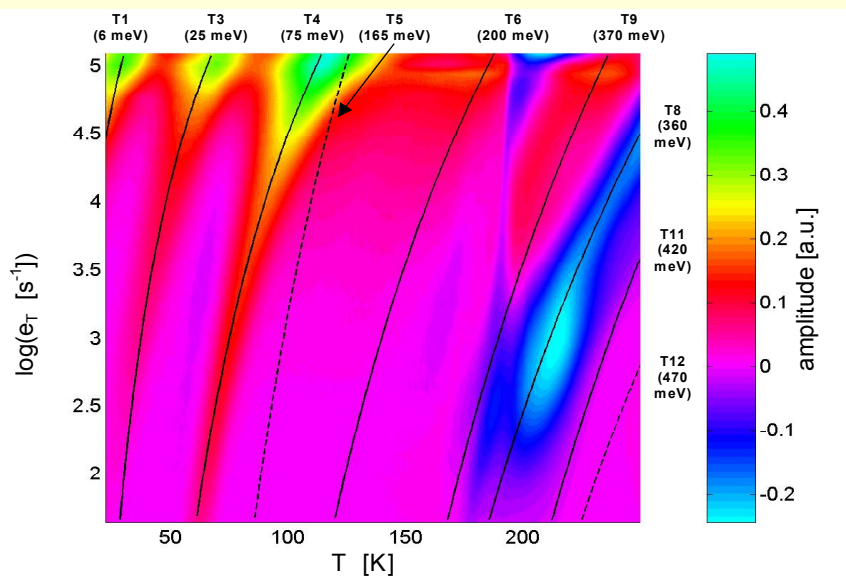


Effect of proton fluence on  $\mu\tau$  of epitaxial Si

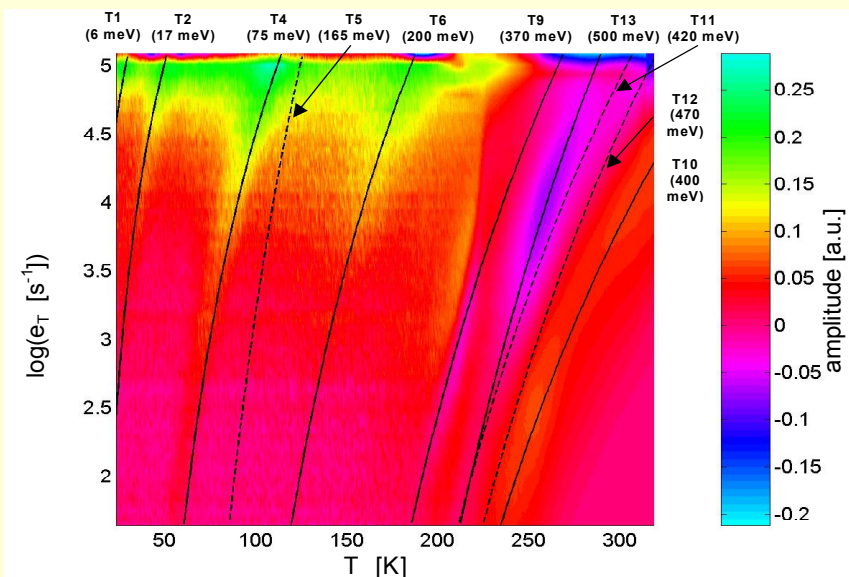
Effect of proton fluence on  $E_{TDDC}$  of epitaxial Si

# Photoinduced transient spectroscopy - Effect of proton fluence on defect structure of epitaxial silicon

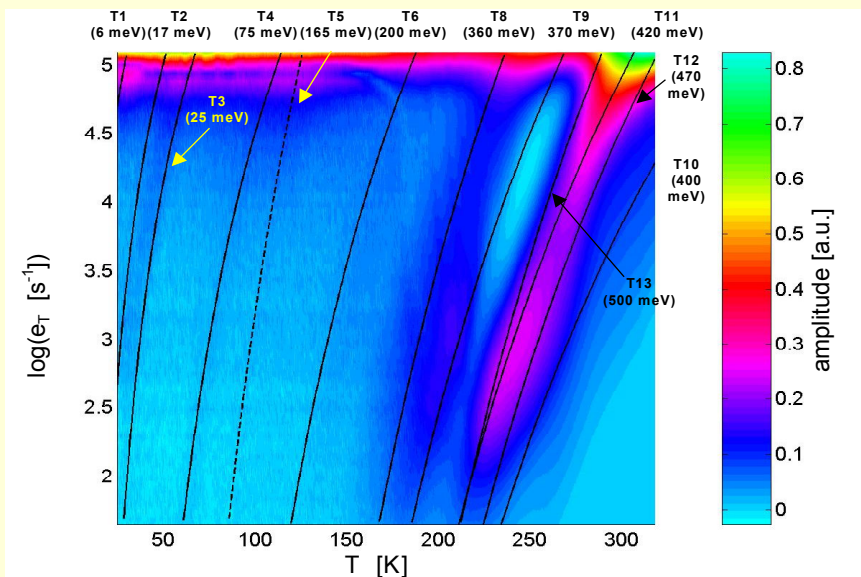
Sample A  $\Phi=1.06 \times 10^{14}$  p/cm<sup>2</sup>



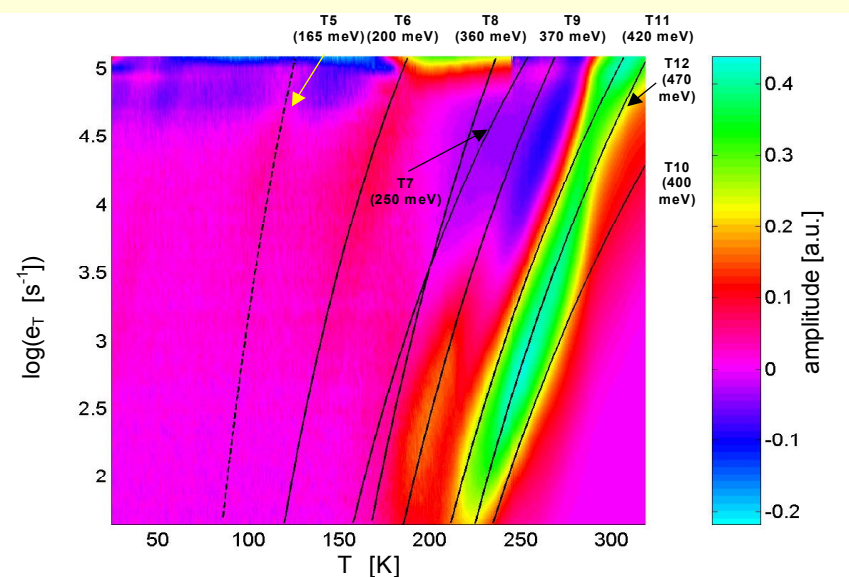
Sample B  $\Phi=5.05 \times 10^{14}$  p/cm<sup>2</sup>



Sample C  $\Phi=2.17 \times 10^{15}$  p/cm<sup>2</sup>



Sample D  $\Phi=6.10 \times 10^{15}$  p/cm<sup>2</sup>



# Photoinduced transient spectroscopy of epitaxial silicon irradiated with high proton fluences

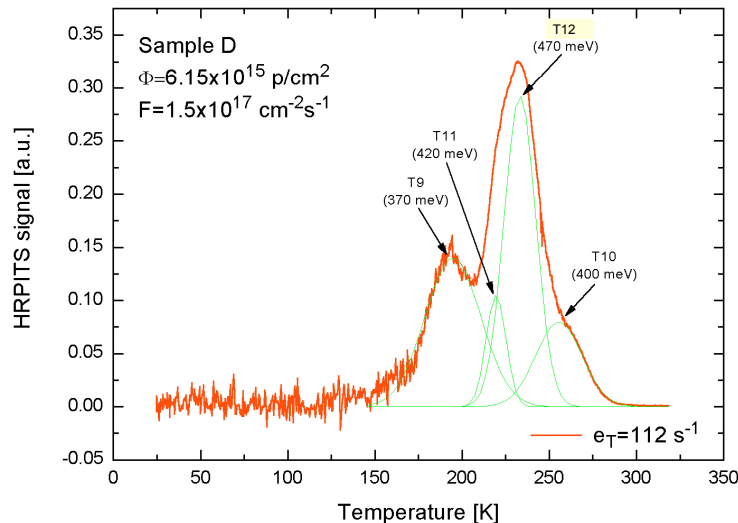
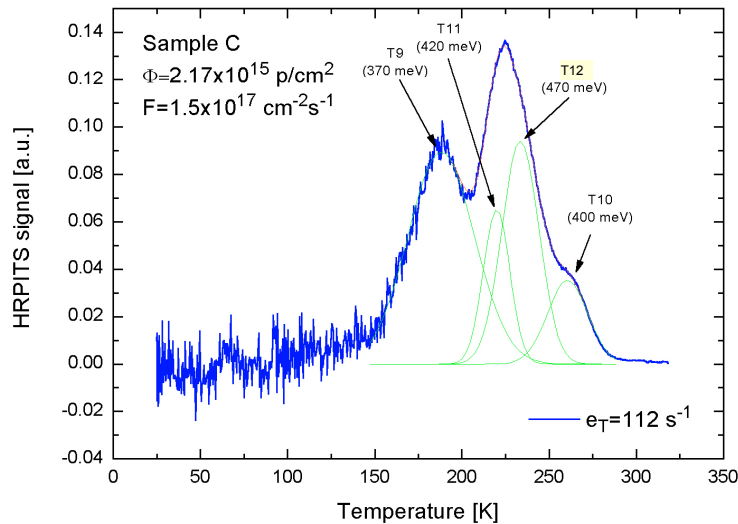
Parameters of defect centres detected by the PITS method in the samples A, B, C and D of epitaxial silicon subjected to 24 GeV/c proton irradiation

Defect centre	Activation energy $E_a$ (meV)	Pre-exponential factor $A$ ( $s^{-1}K^{-2}$ )	Identification
T1	6	$1.5 \times 10^3$	shallow donor
T2	17	$2.2 \times 10^3$	shallow donor
T3	25	$2.4 \times 10^3$	shallow donor
T4	75	$1.8 \times 10^4$	interstitial related ( $I_4$ )
T5	165	$3.0 \times 10^7$	$VO^{-/0}$
T6	200	$8.0 \times 10^5$	$V_2^{0/+}$
T7	250	$1.7 \times 10^5$	$VOH^{+/0}$
T8	360	$1.0 \times 10^8$	$VOH^{-/0}$
T9	370	$1.5 \times 10^7$	$C_iP_s$
T10	400	$8.7 \times 10^5$	$C_iO_i$
T11	420	$1.0 \times 10^7$	$V_2^{0/-}$
T12	470	$3.0 \times 10^7$	$V_2O$
T13	500	$7.6 \times 10^8$	hydrogen related ( $V_2H$ ?)



# Photoinduced transient spectroscopy of epitaxial silicon irradiated with high proton fluences

## The effect of proton fluence on trap concentrations



Defect centre	Activation energy $E_a$ (meV)	Pre- exponential factor $A$ ( $\text{s}^{-1}\text{K}^{-2}$ )	Trap concentration ( $\times 10^{15} \text{ cm}^{-3}$ )	
			Sample C	Sample D
T9	370 ( $\text{C}_i\text{P}_s$ )	$1.5 \times 10^7$	0.14	0.12
T10	400 ( $\text{C}_i\text{O}_i$ )	$8.7 \times 10^5$	3.7	3.3
T11	420 ( $\text{V}_2^{0/-}$ )	$1.0 \times 10^7$	9.9	21.2
T12	470 ( $\text{V}_2\text{O}$ )	$3.0 \times 10^7$	7.9	21.7

Concentration of shallow donors in sample A ( $\Phi=1.06 \times 10^{14} \text{ p/cm}^2$ ) :

- T1 (6 meV) -  $5.0 \times 10^{12} \text{ cm}^{-3}$ ,
  - T2 (25 meV) -  $2.3 \times 10^{13} \text{ cm}^{-3}$  and
- concentration of interstitial related defect
- T4 (75 meV) -  $2.1 \times 10^{14} \text{ cm}^{-3}$

# Effect of proton fluence on formation of defect centres in epitaxial silicon-

## Summary of results

- The irradiation with proton fluences of  $1.06 \times 10^{14}$ ,  $5.05 \times 10^{14}$ ,  $2.17 \times 10^{15}$  and  $6.10 \times 10^{15}$  p/cm<sup>2</sup> results in shifting the Fermi-level position to 0.40, 0.44, 0.57 and 0.59 eV, respectively.
- Apart from typical radiation-induced point defects in Si such as: shallow donors,  $\text{VO}^{-/0}$ ,  $\text{V}_2^{0/+}$ ,  $\text{C}_i\text{P}_s$ ,  $\text{C}_i\text{O}_i$ ,  $\text{V}_2^{0/-}$  and  $\text{V}_2\text{O}$ , some hydrogen related defects as well as an interstitial related defect have been found.
- With increasing the fluence from  $2.17 \times 10^{15}$  to  $6.17 \times 10^{15}$  p/cm<sup>2</sup> the concentrations of  $\text{V}_2^{0/-}$  and  $\text{V}_2\text{O}$  rise from  $1.0 \times 10^{16}$  to  $2.12 \times 10^{16}$  cm<sup>-3</sup> and from  $8.0 \times 10^{15}$  to  $2.17 \times 10^{16}$  cm<sup>-3</sup>, respectively.
- The concentrations of  $\text{C}_i\text{P}_s$  and  $\text{C}_i\text{O}_i$  are of the order  $1.0 \times 10^{14}$  and  $3.0 \times 10^{15}$ , respectively, and are not affected by the increase of proton fluence from  $2.17 \times 10^{15}$  to  $6.17 \times 10^{15}$  p/cm<sup>2</sup>.

# Conclusions

- High-resolution photoinduced transient spectroscopy, based on measurements of photocurrent relaxation waveforms, is an effective tool for studying electronic properties of point defects formed in silicon by irradiation with high-energy particles. The technique is of high sensitivity and allows for monitoring changes in the material defect structure caused by various particle energy and fluence.
- HRPITS technique with implementation of two-dimensional analysis of photocurrent relaxation waveforms has been employed to studying the effect of fluence on defect structure of high purity Cz and FZ silicon irradiated with 10-MeV protons, as well as on defect structure of epitaxial silicon exposed to irradiation with 24 GeV/c protons.
- The irradiation of Cz-Si with fluences of  $1.8 \times 10^{13}$  and  $1.2 \times 10^{14}$  p/cm<sup>2</sup> resulted in the formation of **12** and **14** defect centres, respectively, with activation energies ranging from 15 to 430 meV.
- The irradiation of FZ-Si with fluences of  $1.8 \times 10^{13}$  and  $1.2 \times 10^{14}$  p/cm<sup>2</sup> resulted in the formation of **10** radiation defects with activation energies ranging from 17 to 470 meV and **16** defects with activation energies in the range of 17-597 meV, respectively.
- In epitaxial silicon, apart from typical radiation-induced point defects in Si such as: shallow donors,  $\text{VO}^{-/0}$ ,  $\text{V}_2^{0/+}$ ,  $\text{C}_i\text{P}_s$ ,  $\text{C}_i\text{O}_i$ ,  $\text{V}_2^{0/-}$  and  $\text{V}_2\text{O}$ , a shallow defect T 4 (75 meV), presumably related to interstitials, and a deep defect T 13 (500 meV), tentatively attributed to a complex involving hydrogen, have been found.

# Acknowledgement

**The contribution of E. Nossarzewska-Orłowska, R. Kozłowski, M. Pawłowski, E. Fretwurst, J. Harkonen and E. Tuovinen to obtaining the presented results is greatly acknowledged.**

This work was carried out within the framework of the RD 50 project with financial support of the Polish Ministry of Science and Higher Education under grant No. DWM/40/CERN/2005.